

# Positron Polarization at the International Linear Collider

P. Osland

*CERN, CH-1211 Geneva 23, Switzerland and University of Bergen, N-5007 Bergen, Norway*

N. Paver

*University of Trieste and INFN, I-34100 Trieste, Italy*

We review some recent arguments supporting the upgrade of the International Linear Collider by a polarized positron beam, in addition to the polarized electron beam. The examples presented here mainly focus on the impact of positron polarization on items relevant to new physics searches, such as the identification of novel interactions in fermion-pair production and the formulation of new CP-sensitive observables. In particular, in addition to the benefits from positron and electron longitudinal polarizations, the advantages in this field of having transverse polarization of both beams are emphasized.

## 1. INTRODUCTION

Electron beam longitudinal polarization at the SLC has been a really powerful tool to test the structure of the Standard Model (SM) electroweak interactions and to make precise measurements of the relevant parameters, in particular of the electroweak mixing angle through the left-right asymmetry. No doubt the electron beam with high degree of polarization, already foreseen, will play a similar important rôle at the International Linear Collider (ILC). In addition to scrutinizing the SM dynamics, it should enhance the experimental sensitivity to new physics (NP), which is considered as one of the major parts of the physics programme at this machine. The new physics (NP) might manifest itself either directly *via* the production of new particles whose properties and quantum numbers must be tested, or indirectly through small deviations of cross sections from the SM predictions caused by novel interactions mediated by very heavy states whose couplings must be determined (or constrained) in precision measurements.

In this regard, the full potential of the International Linear Collider could be exploited only with the additional facility of a polarized positron beam. Firstly, at a given annual luminosity, polarized cross sections would be enhanced, in particular an effective polarization larger than the individual  $e^-$  and  $e^+$  polarizations can be defined and more accurately determined. This would greatly increase the sensitivity to small, non-standard, cross sections or to deviations from the SM cross sections. Secondly, the efficiency for chasing non-standard particles (such as, for example, the SUSY particles or the Kaluza-Klein gravitons) could be dramatically improved by strong SM background suppression accompanied by signal enhancement, as allowed by appropriately tuning electron and positron polarizations. Finally, more transition amplitudes and corresponding polarized observables could be defined, which would allow to disentangle the independent components of the novel interactions' multi-parameter space and explore it in detail *via* largely model-independent approaches.

A strong case can also be made for the opportunity of having both beams transversely polarized, which should be realized by the application of spin rotators to the longitudinally polarized beams. By providing the possibility of measuring new (azimuthal) angular distributions and asymmetries, this would extend substantially the potential of searches for novel sources of CP violation and of anomalous triple gauge couplings, as well as to discriminate among models of gravity in extra dimensions. The coordinate system, as well as the angles defining transverse polarization (longitudinal polarization is directed along the  $e^+ - e^-$  axis), are shown in Fig. 1. The examples exposed in the sequel are taken from the exhaustive report on the physics potential of the ILC with both electron and positron beams polarized [1].

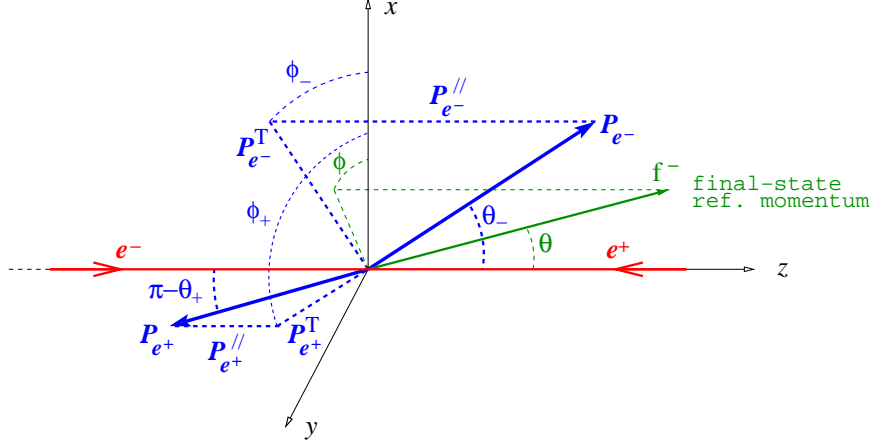


Figure 1: Coordinate system used for momenta and polarization vectors.

## 2. TOP-QUARK FLAVOUR CHANGING NEUTRAL COUPLINGS

FCN *top* couplings are predicted in numerous SM extensions, and therefore represent an interesting field in NP searches, also because they can only occur in the SM through strongly GIM suppressed loops. The  $t \rightarrow Vq$  transitions, with  $V = \gamma, Z$  and  $q = u, c$ , are generally described by an effective interaction, comprising both  $\gamma_\mu$ - and  $\sigma_{\mu\nu}$ -couplings, see for example [2]. Reactions sensitive to FCN couplings are either  $t\bar{t}$  production  $e^+e^- \rightarrow t\bar{t} \rightarrow VqW^-\bar{b}$ , or single top production  $e^+e^- \rightarrow \bar{t}q \rightarrow W^-\bar{b}q$ . Examples of the three- $\sigma$  reach on FCN *top* branching ratios obtainable with different longitudinal beam polarization and with c.m. energy and time-integrated luminosity  $E_{\text{c.m.}} = 0.5$  TeV,  $\mathcal{L}_{\text{int}} = 300 \text{ fb}^{-1}$  and  $E_{\text{c.m.}} = 0.8$  TeV,  $\mathcal{L}_{\text{int}} = 500 \text{ fb}^{-1}$ , are reported in Tab. I [2, 3]. The improvement from  $e^+$  polarization is significant. Comparing with hadron colliders, the LHC (with limits foreseen in the  $10^{-5}$  range) and the ILC may be considered as complementary, with the ILC superior in the discovery reach on  $\sigma_{\mu\nu}$ -couplings [3].

Table I:  $3\sigma$  limits on FCN top branching ratios

| [ $10^{-4}$ ]     |                                | $E = 500$ GeV | $E = 500$ GeV | $E = 500$ GeV | $E = 800$ GeV |
|-------------------|--------------------------------|---------------|---------------|---------------|---------------|
|                   |                                | unpol         | (80%,0)       | (80%,45%)     | (80%,60%)     |
| $\gamma_\mu$      | BR( $t \rightarrow Zq$ )       | 6.1           | 3.9           | 2.2           | 1.9           |
| $\sigma_{\mu\nu}$ | BR( $t \rightarrow Zq$ )       | 0.48          | 0.31          | 0.17          | 0.07          |
| $\gamma_\mu$      | BR( $t \rightarrow \gamma q$ ) | 0.30          | 0.17          | 0.093         | 0.038         |

## 3. CP-VIOLATION IN 3- AND 4-JET Z-BOSON DECAYS

This sector is promising for searches of new CP-violation sources at the GigaZ option, due to the SM being extremely suppressed there, and particularly appealing are the transitions  $Z \rightarrow \bar{b}bg$  and  $Z \rightarrow \bar{b}bgg$ , leading to 3-jet and 4-jet final states ( $g$  denotes the gluon) owing to the excellent  $b$  (and  $\bar{b}$ ) tagging expected at the ILC. A model-independent parameterization of such processes can be obtained by the effective Lagrangian

$$\mathcal{L}_{\text{CP}} = [h_{Vb} \bar{b}T^a\gamma^\nu b + h_{Ab} \bar{b}T^a\gamma^\nu\gamma_5] Z^\mu G_{\mu\nu}^a,$$

with  $T^a$  the color matrices and  $G_{\mu\nu}^a$  the familiar gluon field-strength tensor. Dimensionless constants  $\hat{h}_{Vb}$  and  $\hat{h}_{Ab}$  can be defined out of  $h_{Vb}$  and  $h_{Ab}$  by essentially using  $m_Z^2$  as a scale parameter. Different new physics models

envisage the coupling constants  $h_{Vb}$  and  $h_{Ab}$ , in particular the quark-substructure scenario

$$\mathcal{L}' = \frac{e}{2 \sin \theta_W \cos \theta_W} Z_\mu \bar{b}' \gamma^\mu (g'_V - g'_A \gamma_5) b - i \frac{g_s}{2m_{b'}} \hat{d}_c \bar{b}' \sigma^{\mu\nu} \gamma_5 T^a b G_{\mu\nu}^a + \text{h.c.}$$

Here,  $g'_V$ ,  $g'_A$  and  $\hat{d}_c$  are (in principle complex) constants expected of order unity according to compositeness arguments,  $b'$  denotes a  $b$ -quark excitation and it is understood that  $m_{b'} \gg m_Z$ . The constants  $\hat{h}_{Vb}$  and  $\hat{h}_{Ab}$  are determined by virtual  $b'$  exchange. One can define different CP asymmetries, such as  $T_{33} = (\hat{\mathbf{k}}_{\bar{b}} - \hat{\mathbf{k}}_b)_3 (\hat{\mathbf{k}}_{\bar{b}} \times \hat{\mathbf{k}}_b)_3$  and  $V_3 = (\hat{\mathbf{k}}_{\bar{b}} \times \hat{\mathbf{k}}_b)_3$ , where ‘3’ corresponds to the  $e^+$  direction [4]. We show in Tab. II the one- $\sigma$  accuracy obtainable at the ILC from  $V_3$  on the relevant dimensionless constant  $\hat{h}_b$  from  $Z \rightarrow 3$ -jet events [4]. With both beams polarized,

Table II: Accuracy on  $\hat{h}_b$  and lower limits on  $m_{b'}$

| $V_3$                       | $y_{\text{cut}}$ | $(P_{e^-}, P_{e^+})$ |           |           |              |              |
|-----------------------------|------------------|----------------------|-----------|-----------|--------------|--------------|
|                             |                  | (0, 0)               | (+80%, 0) | (-80%, 0) | (+80%, -60%) | (-80%, +60%) |
| $\tilde{h}_b$ [ $10^{-3}$ ] | 0.01             | 8.5                  | 2.5       | 1.9       | 1.8          | 1.4          |
|                             | 0.1              | 9.5                  | 3.0       | 2.1       | 2.0          | 1.5          |
| $m_{b'}$ [TeV]              | 0.01             | 0.9                  | 1.6       | 1.9       | 2.0          | 2.2          |
|                             | 0.1              | 0.9                  | 1.5       | 1.8       | 1.9          | 2.1          |

the existing sensitivity from LEP is improved by about an order of magnitude, and also the bounds on  $m_{b'}$  are significant, current limits on quark excitations being quite poor.

## 4. MODEL-INDEPENDENT CONTACT INTERACTION SEARCHES

Contact interactions (CI) are used as ‘‘low energy’’ representations of NP dynamics characterized by exchanges of objects with mass scales  $\Lambda$  (much) heavier than the available c.m. energy, that can accordingly be signalled only indirectly, *via* deviations of cross sections from the SM predictions. For  $e^+e^- \rightarrow \bar{f}f$ , we consider the effective, dimension-6 contact interaction Lagrangian [5]

$$\mathcal{L}_{\text{CI}} = \frac{1}{1 + \delta_{ef}} \sum_{i,j=L,R} \frac{4\pi\eta_{ij}}{\Lambda_{ij}^2} (\bar{e}_i \gamma_\mu e_i) (\bar{f}_j \gamma^\mu f_j),$$

with  $|\eta_{ij}| = 1, 0$ . Although originally inspired by fermion compositeness remnant binding forces, this current-current CI may well-represent new physics induced by exchanges of objects heavier than  $\sqrt{s}$  and  $\sqrt{|t|}$  of the process under consideration, for example  $Z$ 's and leptoquarks. In general,  $\sigma$  and  $A_{\text{FB}}$  depend on all CI couplings, unless one considers specific models where only one of them is assumed non-zero. Longitudinal polarization of both beams allows the definition of more observables, and is therefore decisive to perform a model-independent data analysis where the different couplings can be considered as simultaneously non-zero independent free parameters and yet be separately tested or constrained. The resulting 95% C.L. separate reaches on the mass scales  $\Lambda$ , obtainable from the  $\bar{b}b$  and  $\bar{c}c$  channels at the ILC with  $E_{\text{c.m.}} = 0.5$  TeV as a function of the luminosity, are shown in Fig. 2 [6]. Thin lines represent there  $(|P_{e^-}|, |P_{e^+}|) = (80\%, 0)$ , while thick lines represent  $(|P_{e^-}|, |P_{e^+}|) = (80\%, 60\%)$ . The great impact of positron polarization is evident in this figure (for related model-dependent analyses see [7]).

## 5. TRANSVERSELY POLARIZED BEAMS

For the reaction  $e^+e^- \rightarrow \bar{f}f$ , with  $\mathbf{p}$  and  $\mathbf{k}$  the momenta of the  $e^-$  and  $f$  momenta, one can write the transversely polarized differential cross section as

$$\begin{aligned} d\sigma_{\text{pol}} = & A_1 [\mathbf{P}_{e^+}^T \cdot \mathbf{k} + \mathbf{P}_{e^-}^T \cdot \mathbf{k}] + A_2 [\mathbf{P}_{e^+}^T \cdot \mathbf{k} - \mathbf{P}_{e^-}^T \cdot \mathbf{k}] + B (\mathbf{P}_{e^+}^T \cdot \mathbf{P}_{e^-}^T) + C (\mathbf{P}_{e^+}^T \cdot \mathbf{k}) (\mathbf{P}_{e^-}^T \cdot \mathbf{k}) + D (\mathbf{P}_{e^+}^T \times \mathbf{P}_{e^-}^T) \cdot \mathbf{p} \\ & + E_1 [(\mathbf{P}_{e^+}^T \times \mathbf{k}) \cdot \mathbf{p}] (\mathbf{P}_{e^-}^T \cdot \mathbf{k}) + E_2 [(\mathbf{P}_{e^-}^T \times \mathbf{k}) \cdot \mathbf{p}] (\mathbf{P}_{e^+}^T \cdot \mathbf{k}) \end{aligned}$$

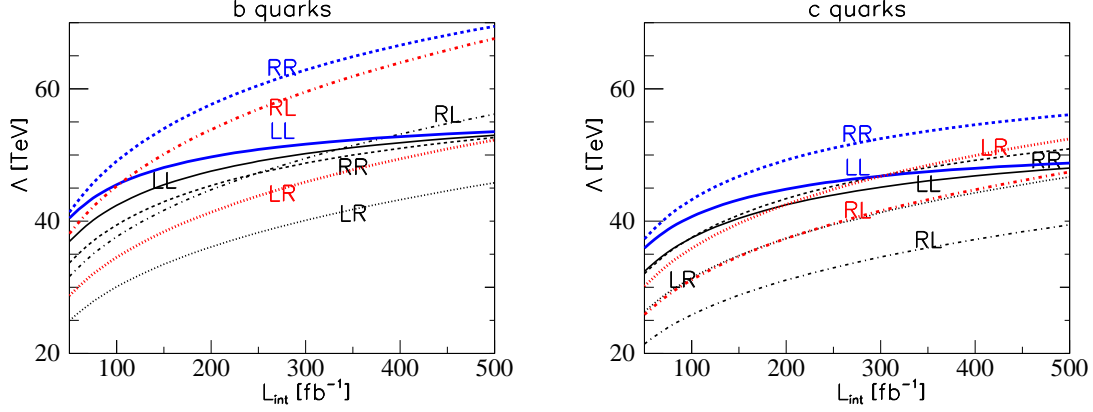


Figure 2: 95% C.L. lower bounds on the CI mass scales  $\Lambda$ .

It can be easily seen that the terms  $A, D$  and  $E$  violate  $P$  and, with reference to Fig. 1, the terms  $B$  and  $C$  combine to give a dependence  $\propto |\mathbf{P}_{e^-}^T| |\mathbf{P}_{e^+}^T| \sin^2 \theta \cos(2\phi - \phi_- - \phi_+)$ , while the  $E$  terms give the dependence  $\propto |\mathbf{P}_{e^-}^T| |\mathbf{P}_{e^+}^T| \sin^2 \theta \sin(2\phi - \phi_- - \phi_+)$ . Clearly, the advantage of transverse polarization is that either  $\mathbf{P}_{e^+}^T$  or  $\mathbf{P}_{e^-}^T$  provides a new direction, and this allows measuring CP violation without (sometimes complicated) final-state spin analyses. Also, with only  $(V, A)$  couplings, the  $A$  terms linear in the transverse polarizations vanish for  $m_e \rightarrow 0$  [8].

## 5.1. New sources of CP-violation

Unconventional interactions in  $e^+e^- \rightarrow \bar{t}t$  can be mediated by (pseudo)-scalar or tensor effective *top* quark couplings. Such new, helicity changing, currents can at the leading order interfere with the SM  $s$ -channel  $(V, A)$   $\gamma$  and  $Z$  exchanges also as  $m_e \rightarrow 0$ , and allow the definition of CP-odd observables that can be measured if transverse beam polarization is available [9]. One can introduce an effective Lagrangian representation of these new interactions in terms of a (high) mass scale  $\Lambda$  and dimension-6 four-fermion operators  $\mathcal{O}_k$  times coefficients  $\alpha_k$  of order unity. The relevant piece, to be added to the SM interaction, can be represented as:

$$\mathcal{L}^{4F} = \frac{1}{\Lambda^2} \sum_k (\alpha_k \mathcal{O}_k + \text{h.c.}) = \sum_{i,j=L,R} \left[ S_{ij} (\bar{e} P_i e) (\bar{t} P_j t) + V_{ij} (\bar{e} \gamma_\mu P_i e) (\bar{t} \gamma^\mu P_j t) + T_{ij} \left( \bar{e} \frac{\sigma_{\mu\nu}}{\sqrt{2}} P_i e \right) \left( \bar{t} \frac{\sigma^{\mu\nu}}{\sqrt{2}} P_j t \right) \right] + \text{h.c.}$$

Here,  $P_i = \frac{1}{2}(1 \pm \gamma_5)$  and  $S_{ij}$ , *etc.* are a priori complex constants. Up-down CP-odd asymmetries in the azimuthal angle  $\phi$  can be constructed, for example the one essentially sensitive to  $\text{Im}S_{RR}$  [9]:

$$A(\theta_0) = \frac{1}{\sigma^{+-}} \int_{-\cos\theta_0}^{\cos\theta_0} d\cos\theta \left[ \int_0^\pi \frac{d\sigma^{+-}}{d\Omega} d\phi - \int_\pi^{2\pi} \frac{d\sigma^{+-}}{d\Omega} d\phi \right],$$

where the superscripts denote aligned opposite transverse polarizations of  $e^-$  and  $e^+$ , and  $\theta_0$  defines a cut-off around the beam directions. The 90% C.L. sensitivity on  $\text{Im}S$  for  $E_{c.m.} = 0.5$  TeV,  $\mathcal{L}_{\text{int}} = 500$  fb $^{-1}$  and full (i.e., 100%) transverse polarization, can be as low as  $10^{-3}$ , which translates to the mass scale  $\Lambda \sim 8$  TeV.

Another representative example of the benefits of positron and electron transverse polarization is the search for anomalous, CP-violating  $\gamma\gamma Z$  and  $\gamma ZZ$  couplings in the production process  $e^+e^- \rightarrow \gamma Z$  at the ILC. In this case,  $(V, A)$  couplings of the (self-conjugate)  $\gamma$  and  $Z$  occur both in the  $s$ - and in the  $t$ -channel, and with transverse polarization CP-odd interference of anomalous couplings with the SM ones is allowed to occur. One can define the anomalous vertex in terms of, a priori complex, couplings  $\lambda_1$  and  $\lambda_2$  as follows [10]:

$$\mathcal{L} = e \frac{\lambda_1}{2m_Z^2} F_{\mu\nu} (\partial^\mu Z^\lambda \partial_\lambda Z^\nu - \partial^\nu Z^\lambda \partial_\lambda Z^\mu) + \frac{e}{16c_W s_W} \frac{\lambda_2}{m_Z^2} F_{\mu\nu} F^{\nu\lambda} (\partial^\mu Z_\lambda + \partial_\lambda Z^\mu).$$

Table III: 90% C.L. limits on anomalous couplings  $\lambda_1$  and  $\lambda_2$ 

| Coupling       | Individual limit from |                      |                      | Simultaneous limits  |
|----------------|-----------------------|----------------------|----------------------|----------------------|
|                | $A_1$                 | $A_2$                | $A_3$                |                      |
| Re $\lambda_2$ | $1.4 \times 10^{-2}$  |                      |                      |                      |
| Im $\lambda_1$ |                       | $6.2 \times 10^{-3}$ | $3.8 \times 10^{-3}$ | $7.1 \times 10^{-3}$ |
| Im $\lambda_2$ |                       | $9.1 \times 10^{-2}$ | $3.0 \times 10^{-2}$ | $6.7 \times 10^{-2}$ |

Interference terms in the photon angular distribution depend on  $\text{Re}\lambda_1$ ,  $\text{Re}\lambda_2$  and  $\text{Im}\lambda_2$ , and are proportional to the product of electron and positron transverse polarizations (parallel polarization directions can be assumed). These couplings can be tested by appropriately defined CP-odd asymmetries, that exploit the dependences  $\sim \cos\theta \cos 2\phi$  and  $\sim \cos\theta \sin 2\phi$  and combine polar forward-backward with azimuthal asymmetries [11]. Explicit expressions can be found in the original references, but it is useful to just mention that, with  $g_V$  and  $g_A$  the familiar SM electron couplings:  $A_1(\theta_0) \propto -\mathbf{P}_{e^-}^T \mathbf{P}_{e^+}^T g_A \text{Re}\lambda_2$ ;  $A_2(\theta_0) \propto \mathbf{P}_{e^-}^T \mathbf{P}_{e^+}^T [(g_V^2 - g_A^2) \text{Im}\lambda_1 - g_V \text{Im}\lambda_2]$ ; finally,  $A_3(\theta_0) \propto \frac{\pi}{2} [(g_V^2 + g_A^2) \text{Im}\lambda_1 - g_V \text{Im}\lambda_2] + \mathbf{P}_{e^-}^T \mathbf{P}_{e^+}^T [(g_V^2 - g_A^2) \text{Im}\lambda_1 - g_V \text{Im}\lambda_2]$ . Consequently, taking into account these dependencies, the couplings  $\lambda_1$  and  $\lambda_2$  can in principle be disentangled and tested separately. Notice that the product of electron and positron transverse polarizations enter in the asymmetries. Tab. III shows the 90% C.L. limits obtainable for an optimal cut-off  $\theta_0 = 26^\circ$ ,  $E_{\text{c.m.}} = 0.5$  TeV,  $\mathcal{L}_{\text{int}} = 500 \text{ fb}^{-1}$  and transverse polarizations  $P_{e^-}^T$  and  $P_{e^+}^T$  equal to 80% and 60%, respectively.

## 5.2. Extra-dimensional gravity in fermion-pair production

Indirect signals of TeV-scale gravity propagating in large, compactified, extra dimensions can be searched for in  $e^+e^- \rightarrow \bar{f}f$ . In the ADD scenario of gravity in extra spatial dimensions [12], the exchange of a tower of Kaluza-Klein (KK) gravitons with almost continuous equally spaced mass spectrum occurs, and can be represented by the dimension-8 effective interaction [13]

$$\mathcal{L}^{\text{ADD}} = i \frac{4\lambda}{M_H^4} T^{\mu\nu} T_{\mu\nu},$$

where  $\lambda = \pm 1$  and  $M_H$  is a cut-off on the summation over the KK states, expected in the TeV range. The  $\cos\theta$ -dependent deviations from the SM, reflecting spin-2 exchange, are proportional to the graviton coupling strength  $f_G = \lambda E_{\text{c.m.}}^4 / (4\pi\alpha_{\text{e.m.}} M_H^4)$ . In the simplest version of the RS scenario [14], space-time is five-dimensional and the (narrow) spin-2 KK resonances can also be in the TeV range but are unequally spaced. Formally, this can be accomplished by the replacement, with  $\Lambda_\pi$  of the TeV order:

$$\frac{\lambda}{M_H^4} \rightarrow \frac{-1}{8\Lambda_\pi^2} \sum_n \frac{1}{s - m_n^2 + im_n\Gamma_n}.$$

Below the production threshold, indirect signals of graviton exchange can be tested, and distinguished e.g. from the four-fermion contact interactions, by using suitable polar asymmetries [15] or differential distributions convoluted with Legendre polynomials [16]. Tab. IV-left shows, as an example, the five- $\sigma$  identification reach on  $M_H$  vs. luminosity, obtainable at the ILC with  $E_{\text{c.m.}} = 0.5$  TeV with longitudinally polarized beams, and combining the  $f = \mu, \tau, c, b$  channels [15]. Clearly, the effect of the additional positron polarization, although being mitigated by the high dimension of the relevant effective operator, helps in increasing the sensitivity to that parameter.

With transverse beam polarization, forward-backward azimuthal asymmetries can be defined [17], but the identification power of such observables on  $M_H$  is similar or less than obtained from longitudinally polarized beams. Tab. IV-center shows the five- $\sigma$  reach from the combination of the  $f = \mu, \tau, c, b$  and  $t$  channels with transverse  $e^-$  and  $e^+$  polarizations of 80% and 60%, respectively.

Table IV: Left: Identification reach on  $M_H$ . Center:  $M_H$  reach. Right: ADD *vs.* RS distinction.

| $M_H$ [TeV]<br>$\sqrt{s} = 0.5$ TeV (long. pol.)        | $\mathcal{L}_{\text{int}}[\text{fb}^{-1}]$ |     |      | $M_H$ [TeV]<br>(transv. pol.) | $\mathcal{L}_{\text{int}}[\text{fb}^{-1}]$ |     |     |      | 5 $\sigma$ disc. reach<br>$M_H$ [TeV] | $\mathcal{L}_{\text{int}}[\text{fb}^{-1}]$ |     |     |      |
|---|--|-----|------|-------------------------------|--|-----|-----|------|---------------------------------------|--|-----|-----|------|
|   | 100  | 300 | 500  |                               | 100  | 300 | 500 | 1000 |                                       | 100  | 300 | 500 | 1000 |
| unpolarised beams                                       | 2.3  | 2.6 | 2.9  | $\sqrt{s} = 0.5$ TeV          | 1.6  | 1.9 | 2.0 | 2.2  | $\sqrt{s} = 0.5$ TeV                  | 1.2  | 1.3 | 1.4 | 1.6  |
| $(\mathbf{P}_{e^-}, \mathbf{P}_{e^+}) = (+80\%, 0)$     | 2.5  | 2.8 | 3.05 | $\sqrt{s} = 0.8$ TeV          | 2.4  | 2.6 | 2.8 | 3.1  | $\sqrt{s} = 0.8$ TeV                  | 1.8  | 2.0 | 2.2 | 2.4  |
| $(\mathbf{P}_{e^-}, \mathbf{P}_{e^+}) = (+80\%, -60\%)$ | 2.45                                       | 3.0 | 3.25 | $\sqrt{s} = 1.0$ TeV          | 2.8  | 3.2 | 3.4 | 3.8  | $\sqrt{s} = 1.0$ TeV                  | 2.2  | 2.4 | 2.6 | 2.8  |

Conversely, with transverse polarization, discrimination among ADD and RS gravity scenarios is possible, by means of the azimuthal asymmetry between events at positive and negative values of  $\sin 2\phi$  [17]:

$$\frac{1}{N} \frac{dA_i^T}{d \cos \theta} = \frac{1}{\sigma} \left[ \int_+ \frac{d\sigma}{d \cos \theta d\phi} - \int_- \frac{d\sigma}{d \cos \theta d\phi} \right].$$

While vanishing for both the SM and the RS resonance cases (neglecting widths with respect to masses), this asymmetry receives a finite contribution in the ADD scenario, through an imaginary part that can be acquired by the graviton coupling constant  $f_G$ . Tab. IV-right shows the corresponding ADD *vs.* RS five- $\sigma$  discrimination power at the ILC, for the same input values as in Tab. IV-center.

## Acknowledgments

Research supported in part by the Research Council of Norway, Trieste University and MIUR.

## References

- [1] G. Moortgat-Pick *et al.*, arXiv:hep-ph/0507011.
- [2] J. A. Aguilar-Saavedra and T. Riemann, arXiv:hep-ph/0102197.
- [3] E. W. N. Glover *et al.*, Acta Phys. Polon. B **35**, 2671 (2004); J. A. Aguilar-Saavedra, Acta Phys. Polon. B **35**, 2695 (2004).
- [4] O. Nachtmann and C. Schwanenberger, Eur. Phys. J. C **32**, 253 (2004).
- [5] E. Eichten, K. D. Lane and M. E. Peskin, Phys. Rev. Lett. **50** (1983) 811; R. Ruckl, Phys. Lett. B **129** (1983) 363.
- [6] A. A. Babich, P. Osland, A. A. Pankov and N. Paver, Phys. Lett. B **518**, 128 (2001).
- [7] S. Riemann, LC-TH-2001-007
- [8] G. V. Dass and G. G. Ross, Phys. Lett. B **57**, 173 (1975); Nucl. Phys. B **118**, 284 (1977).
- [9] B. Ananthanarayan and S. D. Rindani, Phys. Rev. D **70**, 036005 (2004); Phys. Lett. B **606**, 107 (2005).
- [10] K. J. Abraham and B. Lampe, Phys. Lett. B **326**, 175 (1994).
- [11] B. Ananthanarayan, S. D. Rindani, R. K. Singh and A. Bartl, Phys. Lett. B **593**, 95 (2004) [Erratum-ibid. B **608**, 274 (2005)].
- [12] N. Arkani-Hamed, S. Dimopoulos and G. R. Dvali, Phys. Rev. D **59**, 086004 (1999); I. Antoniadis, N. Arkani-Hamed, S. Dimopoulos and G. R. Dvali, Phys. Lett. B **436**, 257 (1998).
- [13] J. L. Hewett, Phys. Rev. Lett. **82**, 4765 (1999).
- [14] L. Randall and R. Sundrum, Phys. Rev. Lett. **83**, 3370 (1999).
- [15] P. Osland, A. A. Pankov and N. Paver, Phys. Rev. D **68**, 015007 (2003); A. A. Pankov and N. Paver, arXiv:hep-ph/0501170.
- [16] T. G. Rizzo, JHEP **0210**, 013 (2002).
- [17] T. G. Rizzo, JHEP **0302**, 008 (2003).